

NUMERICAL SIMULATION ON THE THERMAL PROCESS OF WAXY CRUDE OIL DURING ITS STORAGE UNDER DIFFERENT WALL TEMPERATURES

by

Jian ZHAO^a, Yanpeng Li^a, Hang DONG^{a*}, Junyang LIU^a, and Dongjie QU^b

^aKey Laboratory of Enhance Oil and Gas Recovery of Educational Ministry,
Northeast Petroleum University, Daqing, China

^bNorth oil depot, Storage, Transportation and Sales Branch, Daqing Oilfield Co. LTD.,
Daqing, China

Original scientific paper
<https://doi.org/10.2298/TSCI210615021Z>

This study aims to elucidate the underlying mechanism of the association between heat characteristics and influencing factors and to provide theoretical guidance for increasing safety and economics during waxy crude oil storage. Physical and mathematical models with the numerical approaches to represent the static cooling of waxy crude oil are established. Based on the numerical simulations, the effect of the wall temperature on the temperature and velocity distribution is mainly confined to the thermal influence region near the wall, and it increases with the cooling process. The gelation of waxy crude oil near the wall is the most significant and highly correlated with the convection heat transfer coefficient near the wall, so both are significantly affected by the wall temperature. In addition, based on the partial correlation and grey correlation analysis, the effect of the wall temperature is quantitatively analysed. The results show that the correlation between wall temperature and average cooling rate is very significant. In contrast, the correlation between sidewall temperature and thermal characteristics and its derived gelation behaviour are more significant. Furthermore, detailed information on the correlation between the wall temperature and the parameters that characterize the thermal characteristics is obtained.

Key words: numerical simulation, waxy crude oil, grey relational analysis, wall temperatures, temperature drop

Introduction

Waxy crude oil makes up a significant portion of China's crude oil reserves and demand. Revealing the heat transfer characteristics and mechanism under various factors during the storage of waxy crude oil and finding out the internal relationship between heat transfer characteristics and various influencing factors can provide theoretical guidance for improving the safety and economy of waxy crude oil storage and transportation.

Busson and Miniscloux [1], a simplified calculation model of crude oil storage tank temperature prediction based on the assumption of fluid homogeneity and mixing is established. Cotter *et al.* [2-4] numerically analyzed the heat flow characteristics of crude oil during normal transportation. Zhao [5-7] used the wavelet finite element method to study the temperature distribution and cooling law of crude oil. Li [8, 9] discusses heat transfer characteristics and

* Corresponding author, e-mail: dh.123@163.com

the influence of solar radiation on crude oil storage tanks, and the influence of insulation layer thickness on thermal mass. In filling the fuel oil storage tank under varying flow velocities and in various instances of heating Vardar [10] investigated the characteristics of flow pattern and the transient temperature distribution. In addition numerical simulation, laboratory simulation or field test is also the main method for studying the characteristics of crude oil storage tank heat transfer. Mawire [11-13] experimented and simulated the thermal mechanism of a small unisolated oil storage tank that suffered heat loss when being charged. The characteristics of thermal gradients in the tank and the influence factors were evaluated in detail. On this basis, the experiments were performed. Under different conditions, the temperature, stratification number, and heat-loss factor profiles were assessed. The temperature and velocity of nearby tank walls in double-deck floating roof tanks are studied by Liu *et al.* [14]. The influence of vapor amount and height of tank wall on temperature field is also analyzed. The thermal characteristics and flow behavior caused by natural-convection were investigated. But the complicated rheological property during the waxy crude oil storage process and the phase change behavior from sol to gel caused by temperature decrease make the heat transfer characteristics more complex during the cooling process. Study findings on the characteristics of thermal transfer during the waxy crude oil process are also relatively few. Wang *et al.* [15-17] performed the test in a 100000 m³ oil tank, in conjunction with the computational simulation of waxy crude oil heat transfer characteristics. During the refraining operation, Zhao *et al.* [18] performed a numerical investigation for the conversion of heat and jelled properties of waxy crude oil.

The objective of this study is therefore, to analyze the influence of boundary conditions on the thermal properties of waxy crude oil through a numerical simulation approach during its static storage operation. The evolution of gelatinization structure, convective heat transfer coefficient at walls, temperature distribution, and flow pattern under various boundary temperatures are thoroughly studied to understand the mechanism of boundary temperatures affecting the heat transfer characteristic. In addition, the influence of boundary temperature is further analyzed quantitatively to provide more meaningful theoretical guidance for engineering practice.

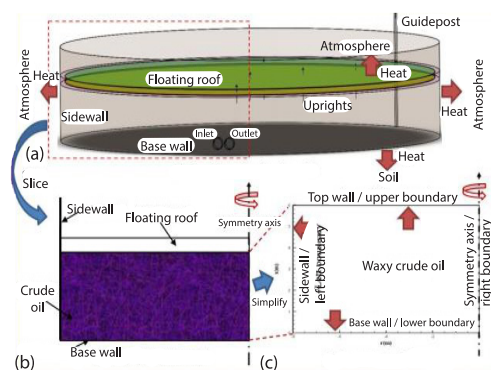


Figure 1. Introduction thermal system; (a) the 3-D tank model, (b) axial symmetry model, and (c) computational domain

thermal properties of waxy crude oil. At the same time, the viscosity of waxy crude oil increases significantly. When this process develops further, with the increase of the amount of paraffin precipitated, the 3-D grid structure of paraffin is generated. The rheological behavior of waxy crude oil changes from Newtonian fluid to non-Newtonian fluid, releasing a large amount of latent heat.

Establishment of the physical model

Heat transfer system and the solve the domain

The establishment process of the physical model and solution domain is shown in fig. 1. The simplification process and description of the model have been described in detail in our previous studies [19].

Waxy crude oil

When the temperature is higher, waxy crude oil is a single-phase system with better fluidity. When the temperature drops to the wax appearance temperature, the paraffin begins to crystallize. In this process, latent heat release affects the

The latent heat caused by the paraffin crystallization is represented by the additional specific heat capacity. The data of specific heat capacity as a function of temperature is measured by DSC (TA Q2000) [19]. However, since the variation of shear rate induced by natural-convection is rather small, the viscosity data as a function of temperature at the low shear rate is used in the simulation. The data of viscosity is measured by rheometer (Anton Paar QC) [19]. The losing flow point temperature of waxy crude oil is 34 °C, while the jelled point temperature is 30 °C. The density is assumed as a constant except in the buoyancy terms of the momentum equations (Boussinesq approximation). The density of crude oil at 20 °C is 850 kg/m³, and the coefficient of thermal expansion is 0.000844 K⁻¹. The thermal conductivity is regarded as a constant with the value of 0.14 W/mK.

Mathematical model, numerical approach, and verification process

Mathematical model

- Flow and heat transfer equation

The continuity equation:

$$\frac{\partial \rho}{\partial t} + \frac{\partial(\rho u)}{\partial x} + \frac{1}{r} \frac{\partial(\rho r v)}{\partial r} = 0 \quad (1)$$

Momentum equation: The movement behavior of waxy crude oil is not only subjected to gravity, friction force and pressure because of the natural-convection in static storage process, but also subjected to the extra resistance caused by formation of wax crystal when oil temperature is lower than losing flow point. As a result, the motion equation of waxy crude oil in the cylindrical co-ordinate can be established:

$$\frac{\partial(\rho u)}{\partial t} + \frac{\partial(\rho u u)}{\partial x} + \frac{1}{r} \frac{\partial(r \rho v u)}{\partial r} = -\frac{\partial p}{\partial x} + \frac{\partial}{\partial x} \left(\mu \frac{\partial u}{\partial x} \right) + \frac{1}{r} \frac{\partial}{\partial r} \left(r \mu \frac{\partial u}{\partial r} \right) - \rho g + S_u \quad (2)$$

$$\frac{\partial(\rho v)}{\partial t} + \frac{\partial(\rho u v)}{\partial x} + \frac{1}{r} \frac{\partial(r \rho v v)}{\partial r} = -\frac{\partial p}{\partial r} + \frac{\partial}{\partial x} \left(\mu \frac{\partial v}{\partial x} \right) + \frac{1}{r} \frac{\partial}{\partial r} \left(r \mu \frac{\partial v}{\partial r} \right) - \frac{\mu v}{r^2} + S_v \quad (3)$$

The additional flow resistance of waxy crude oil is represented by the sink terms of and in the momentum equations. The expressions of 2 and 3 are:

$$S_u = -\frac{(1-\beta)^2}{(\beta^3 + 0.001)} C u, \quad S_v = -\frac{(1-\beta)^2}{(\beta^3 + 0.001)} C v \quad (4)$$

Since the flow resistance of waxy crude oil increases with the temperature drops, the parameter β in the momentum source terms is used to establish the relationship with the temperature, and parameter C is taken as a constant which is used to compromise the flow resistance and the momentum source term [20]. It is believed that when the flow resistance caused by the yield characteristic surpasses the buoyancy force from convection, the waxy crude oil begins to gelatinize. At this moment, the value of parameter β is taken as 0, so the value of parameter C is calculated based on the equivalent relationship between the buoyancy force and flow resistance. The expressions of parameter β :

$$T > T_s, \beta = 1, \quad T < T_z, \beta = 0, \quad T_z < T < T_s, \beta = \frac{T - T_z}{T_s - T_z} \quad (5)$$

Energy equation:

$$\frac{\partial(\rho C_p T)}{\partial t} + \frac{\partial(\rho C_p u T)}{\partial x} + \frac{1}{r} \frac{\partial(r \rho C_p v T)}{\partial r} = \frac{\partial}{\partial x} \left(\lambda \frac{\partial T}{\partial x} \right) + \frac{1}{r} \frac{\partial}{\partial r} \left(r \lambda \frac{\partial T}{\partial r} \right) \quad (6)$$

– Boundary conditions

$$x = H_{\text{tank}}, -R_{\text{tank}} \leq r \leq 0, T_{r,x} = T_{\text{roof}} \quad (7)$$

$$0 \leq x \leq H_{\text{tank}}, r = -R_{\text{tank}}, T_{r,x} = T_{\text{sidewall}} \quad (8)$$

$$x = 0, -R_{\text{tank}} \leq r \leq 0, T_{r,x} = T_{\text{basewall}} \quad (9)$$

$$0 \leq x \leq H_{\text{tank}}, r = 0, -k = \frac{\partial T}{\partial r} = 0 \quad (10)$$

– Initial condition

$$T(r,x) = T_0, u(r,x) = v(r,x) = 0, p = p_0 \quad (11)$$

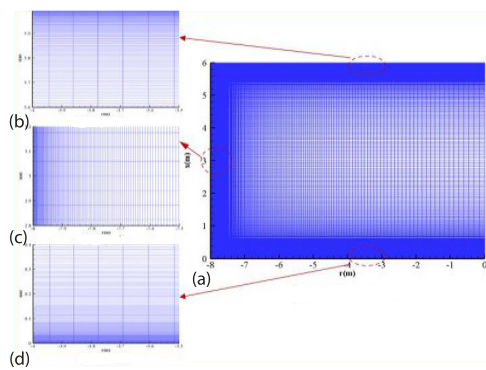


Figure 2. Computational domain discretization; (a) full view of the mash, (b) top wall, (c) sidewall, and (d) base wall

are compared to the experimental results. The findings demonstrate that the computational simulation and experimental results are identical. Between test results and simulation results the total relative error is 1.98%. The relative max error is 3.00% while the relative minimum error is 1.21%.

Results and discussions

Numerical simulation scheme

The basic model and calculation method have been verified, and five working conditions have been designed. The base wall temperature is 30 °C; the sidewall temperature and top wall temperature are 0 °C, 10 °C, and 20 °C, respectively.

Effect of sidewall temperature

Evolution of temperature distribution

In order to further analyze the effect of sidewall temperature on the oil temperature distribution, data of oil temperature near the sidewall is collected in fig. 3.

As shown in fig. 3, in the 240 hours temperature drop process, the temperature differences in the computational domain under different wall temperatures are mainly concentrated in a small region near the sidewall, which can be referred as the thermal influence region (TIR) of sidewall temperature in the computational domain. For different sidewall temperatures, the

Numerical approaches

The governing equations and boundaries are solved using the finite volume method. The computing domain has to be discretized before calculation. The discrete processes of the computational domain and governing equations have been described in detail in [21], so there is no need to repeat them here. The grid details are shown in fig. 2.

Validation of the numerical approaches

In this part, the correctness of the numerical method is verified, and the experimental system used in the verification has been introduced in detail in [20]. The simulation findings

range of TIR and the temperature difference increase with the progress of temperature drop, and the range of TIR increases with the decrease of sidewall temperature. For example, the thickness of TIR is 0.35 m when temperature drop is 280 hours, sidewall temperature is 0 °C and the height is 5 m. While when sidewall temperature is 20 °C and the height is also 5 m, the thickness of TIR is 0.22 m. The oil temperature outside the TIR is not affected by the sidewall temperature, and the evolution of oil temperature is basically the same.

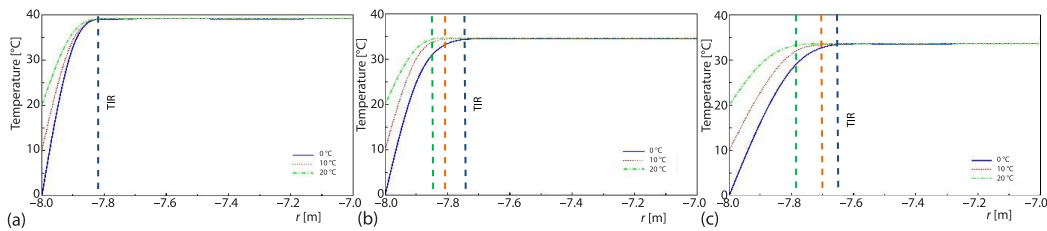


Figure 3. Temperature along the radial direction at different cooling time at $H = 5$ m;
 (a) $t = 4$ hours, (b) $t = 140$ hours, and (c) $t = 240$ hours

Effect of the sidewall temperature on the oil flow

The diagrams in fig. 4 show that the evolution process of the crude oil velocity field in the computational domain is basically the same at different wall temperatures. With increasing cooling time, the viscosity of crude oil increases, and the overall flow velocity decreases. Simultaneously, with the evolution of the temperature field and progress of the gelation process of crude oil, the flow region, which is identical to the high temperature region in the computational domain, gradually decreases. When the temperature drop progresses ($t = 120$ hours), the velocity in the computational domain slightly increases with increasing wall temperature, but the difference in the vortex structure still does not have significant regularity. Comparatively, the influence of the sidewall temperature on the convection field is mainly confined to the TIR near the sidewall. According to fig. 4, a lower sidewall temperature obviously corresponds to a larger space occupied by the low velocity region near the sidewall and a weaker flow intensity.

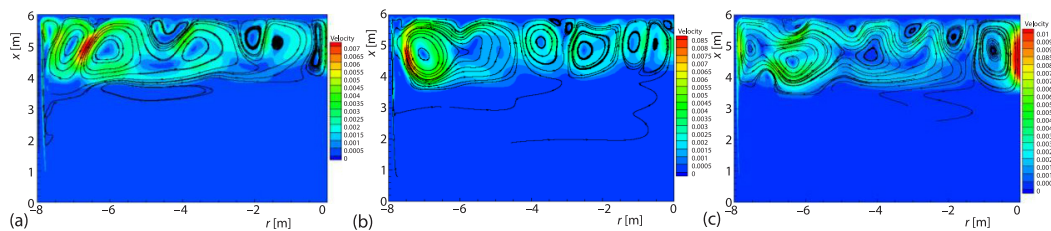


Figure 4. Velocity contour plots at different sidewall temperatures at 120 hours during cooling;
 (a) sidewall temperature is 0 °C, (b) sidewall temperature is 10 °C, and (c) sidewall temperature is 20 °C

Effect of the sidewall temperature on the convective heat transfer coefficient at the walls

Figures 5(a) and 5(b) describe the change in wall convective heat transfer coefficient with the cooling process. The convective thermal coefficient gradually decreases with the cooling time and tends to be stable, which is consistent with the gradual weakening of convection in the storage tank. The results show that the temperature of the sidewall hardly affects the top wall surface. The influence of the sidewall temperature is limited to the local area near

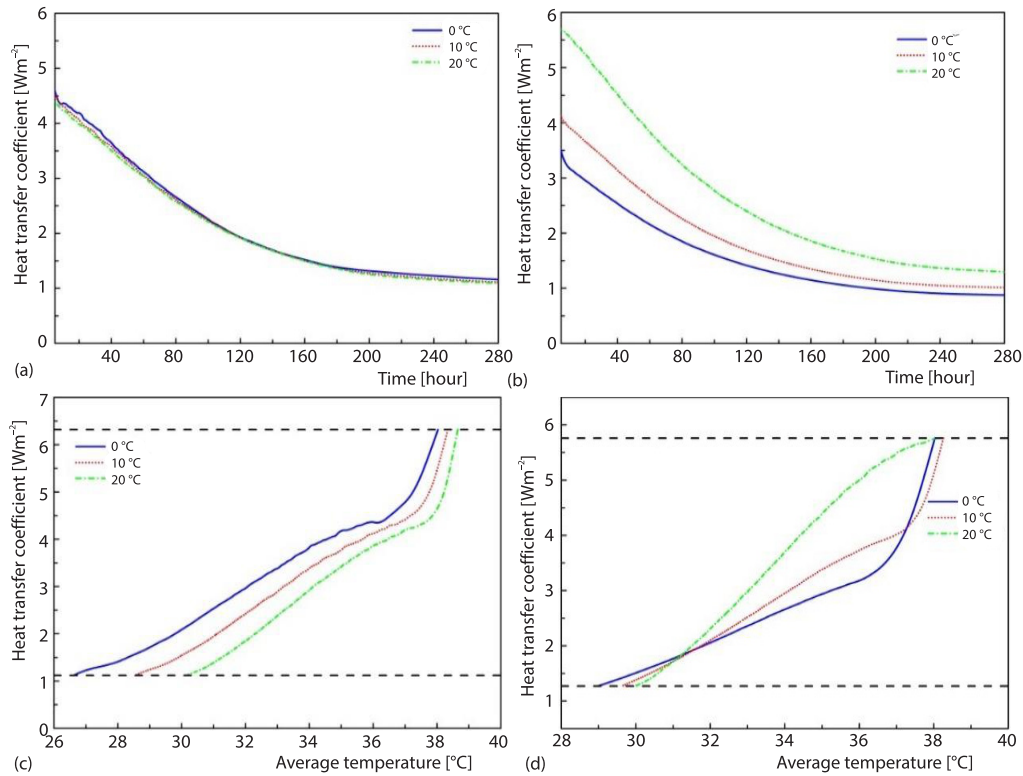


Figure 5. Change in wall convective heat transfer coefficient; (a) at the top wall, (b) at the sidewall, (c) at the top wall, and (d) at the sidewall

the sidewall, which can be referred to as TIR. As shown in fig. 5(b), the sidewall temperature greatly affects the sidewall convective heat transfer. A lower wall temperature increases the oil viscosity near the wall surface, and natural-convection is weakened. Therefore, the resulting convective heat transmission coefficient is weaker if the sidewall temperature is smaller. The wall temperature is a very important factor for oil temperature.

Figure 5(c) describes the variation in convective heat transfer coefficient with the average temperature at different sidewall temperatures. At the same average temperature, a lower wall temperature corresponds to stronger convective heat transfer. The lower top wall temperature enhances the convective heat transfer of the oil near the upper boundary. In addition, the coefficient rapidly and slowly decreases with the change in average temperature, where there is an obvious transition process.

Figure 5(d) shows that the development of the coefficient of sidewall heat transmission is more complex, whereas the coefficient of the top wall convective heat transfer is simple. The change in temperature near the left boundary and the temperature near the upper boundary have opposite effects on the coefficient. The left boundary temperature reduces the temperature differential, and the heat transfer of the fluid near the left boundary is enhanced, but the oil viscosity near the sidewall is increased. As shown in fig. 5(b), when the average temperature is higher than 37.3 °C, the convective heat transfer coefficient is maximal when the sidewall temperature is 20 °C because the oil viscosity is much smaller and the convection is more intense than those in the other two cases. With the decrease in sidewall temperature, the temperature

difference has a larger effect than the oil viscosity. Therefore, the convective heat transfer coefficient when the sidewall temperature is 0 °C is larger than that when the sidewall temperature is 10 °C. However, since the oil cools much faster when the sidewall temperature is lower, the reduction in convective heat transfer coefficient is most significant when the sidewall temperature is 0 °C. Then, with the decrease in oil temperature, the effect of temperature near the sidewall mainly controls the evolution of the convective heat transfer coefficient. Thus, with the decrease in sidewall temperature, the convective heat transfer coefficient decreases. When the average temperature is lower than 31.3 °C, the calculated convective heat transfer coefficients based on the equation are not suitable to represent the intensity of the convection flow because the waxy crude oil has turned into the jelled state. For three cases, the lower sidewall temperature corresponds to a higher centre temperature; thus, the convective heat transfer coefficient for different cases presents an opposite performance.

Effect of wall temperature on the gel layer

Figures 6(a) and 6(b), in the area near the wall, different wall temperatures affect the thickness of the gel layer nearby. However, because the influence on the surface temperature of the sidewall is more direct, the gel thickness around the sidewall changes more obviously. The effect of gel layer thickness on the upper boundary should mainly occur near the sidewall. Comparing the data in figs. 5(b) and 6(b), the effect of sidewall temperature on the thickness of the gel layer is opposite to that on the wall heat transfer coefficient. The larger the temperature difference near the wall, the thicker the gel layer. The formation of the gel layer was significantly affected by wall convection. Figures 6(c) and 6(d) also describes the variation of the gel layer thickness caused by the average temperature in the calculated domain.

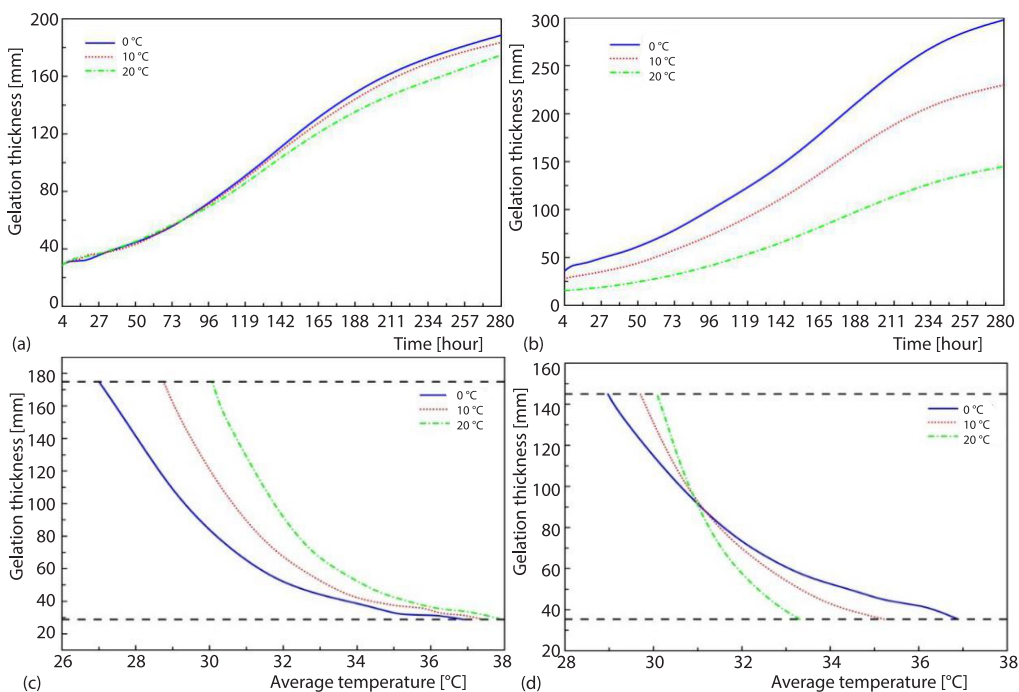


Figure 6. The change of the wall gel layer; (a) at the top wall, (b) at the sidewall, (c) at the top wall, and (d) at the sidewall

As seen in fig. 6(c), while with a rise in the sidewall temperature and the cooling rate decreases, the thickness of the gelatinization layer is increased at the same level of average temperature. Normally, the average temperature is taken as an important criterion for the safety of the tank. Same average temperature, the lower the upper wall temperature is, the thicker the gel layer is. Therefore, the average temperature is not sufficient for the criterion of the safety of the tank. The increase of sidewall temperature cannot prevent the gelatinization progress at the upper boundary. Conversely, at the same average temperature, the higher the wall temperature is, the lower the center temperature will be. The lower center temperature accelerates gelatinization progress at the top wall. Figure 6(d) shows that the gelling of the sidewall is more complicated. When the mean temperature is more than 31 °C, the lower the sidewall temperature is, the thicker the cementitious layer is. Near-wall convection has an impact on the thickness of the gel layer. The smaller the gelatinization layer is, the higher the convective heat transfer coefficient. Comparing the data in figs. 5(d) and 6(d), the evolution of gelatinization layer thickness can be interpreted by this relation. In addition, by comparing the data in two figures, the transition temperature of different performances is the same with the value of 31 °C.

Effect of top wall temperature

Evolution of temperature distribution

As seen in fig. 7, similar to the influence of side wall temperature, the temperature differences in the computational domain under different top wall temperatures are mainly concentrated in a small area near the top wall, which can be referred as the TIR of the top wall temperature. For different top wall temperatures, the range of TIR and the temperature difference increase with the progress of cooling, and the range of TIR increases with the decrease of top wall temperature. For example, the thickness of TIR is 0.35 m at 180th hours during cooling, when top wall temperature is 0 °C and at the radial position $r = -1$. While when top wall temperature is 20 °C, the thickness of TIR is 0.23 m.

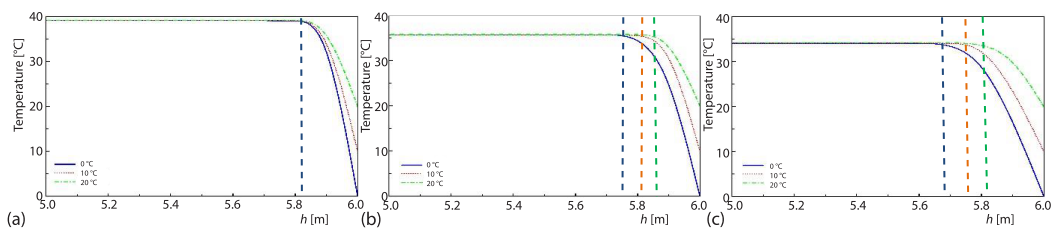


Figure 7. Temperature along the axis direction at different cooling time at $r = -1$;
(a) $t = 20$ hours, (b) $t = 140$ hours, and (c) $t = 180$ hours

Evolution of flow pattern

As shown in fig. 8, the overall characteristics of the crude oil velocity field in the computational domain are basically identical at different top wall temperatures. With the evolution of the temperature field and gelation process of crude oil, the flow region, which is identical to the high temperature region in the computational domain, decreases. When the temperature drops after 120 hours, the velocity value in the computational domain slightly increases with increasing top wall temperature, but the difference in the vortex structure still has no significant regularity, which reflects the randomness of the flow in the computational domain. Comparatively, the influence of the top wall temperature on the convection field is still mainly confined to the TIR near the top wall. According to fig. 8, a lower top wall temperature obviously cor-

responds to a larger space occupied by the low velocity region near the top wall and a weaker flow intensity.

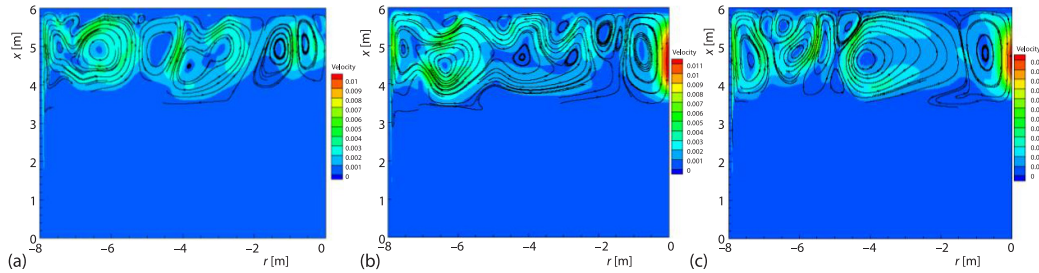


Figure 8. Velocity contour plots at different top wall temperatures at 120 hours during cooling; (a) top wall temperature is 0 °C, (b) top wall temperature is 10 °C, and (c) top wall temperature is 20 °C

Effect of the top wall temperature on the convective heat transfer coefficient at the walls

Figures 9(a)-9(d) show the change in convective heat transfer coefficient on the top wall and sidewall with the average temperature, respectively.

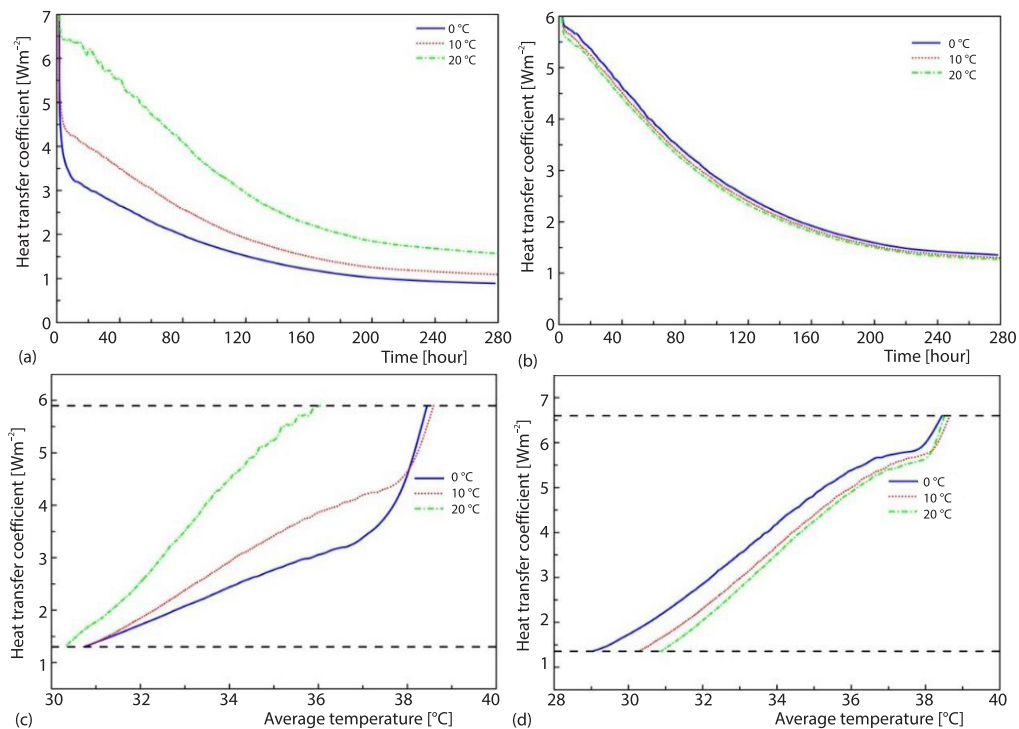


Figure 9. Change in wall convective heat transfer coefficient; (a) at the top wall, (b) at the sidewall, (c) at the top wall, and (d) at the sidewall

Figures 9(a) and 9(b) show that a smaller heat transfer coefficient corresponds to a longer cooling process. The variation in temperature of the top wall does not affect the convective coefficient of heating transfer on the sidewalls, and the convection coefficient of the

sidewall remains stable while the top wall temperature increases or decreases. This result is consistent with the previous conclusion that the top wall temperature only affects a limited area near the top. The convective top wall heat transfer coefficient is significantly influenced by the high wall temperature. For a drop in temperature, the coefficient of the upper boundary more quickly decreases.

Figure 9(d) shows that at the same average temperature, a higher upper boundary temperature corresponds to a smaller convective heat transfer coefficient, which is consistent with previous findings. In addition, the convective heat transfer coefficient at the top wall is more complicated than that at the sidewall. The performance is also similar to that of the convective heat transfer coefficients at the sidewall under different sidewall temperatures. The temperature difference between the oil and the top wall and the average temperature near the top wall have opposite effects on the evolution of the convective heat transfer coefficient, which contributes to the performance in fig. 9(a).

Effect of the top wall temperature on the gel layer

Figures 10(a) and 10(b) show that because of the temperature variation of the upper boundary, the gelation phenomenon in the surrounding area is greatly affected. The temperature increases, and the gel layer becomes smaller. Figures 10(c) and 10(d) describe the evolution of the thickness of the wall gel with the average temperature.

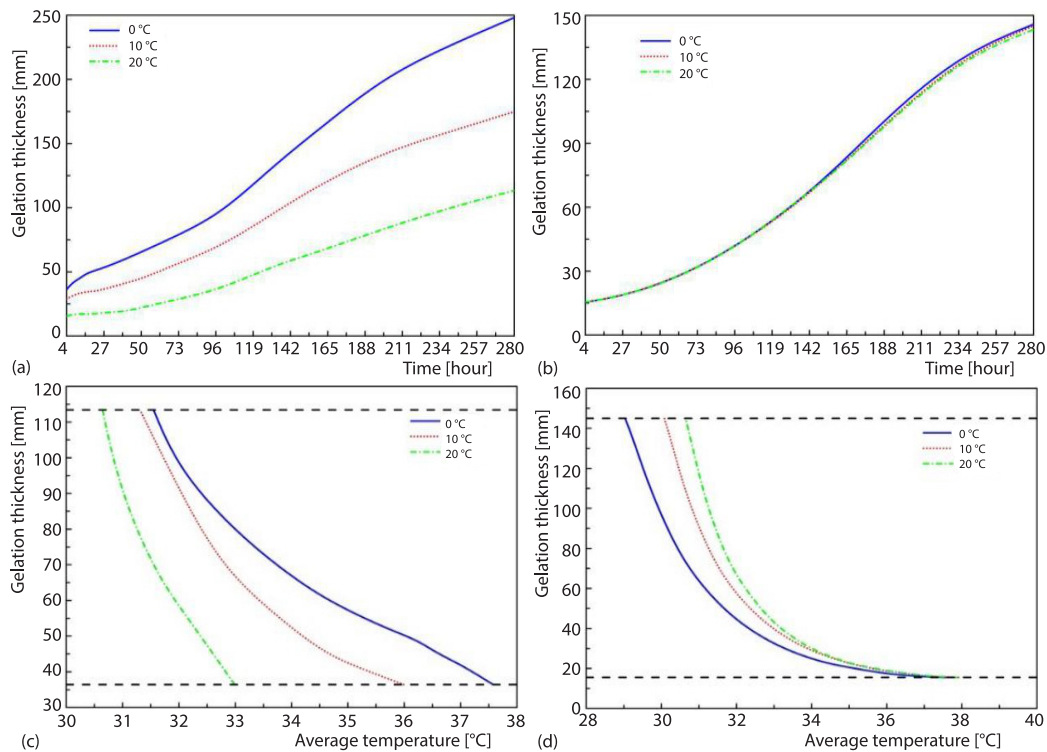


Figure 10. Change in the wall gel layer; (a) at the top wall, (b) at the sidewall, (c) at the top wall, and (d) at the sidewall

As shown in fig. 10(d), at the same average temperature, the gelatinization layer thickness increases with increasing top wall temperature. As discussed in the previous section, the

increase in top wall temperature cannot prevent the thickening progress of the gelatinization layer at the sidewall. With the decrease in top wall temperature, the gelatinization layer thickness increases at the same average temperature. The change in thickness of the gelatinization layer is directly affected by convection near the wall. Thus, a larger convective heat transfer coefficient corresponds to a thinner gelatinization layer.

Mathematical analysis under the influence of wall temperature

The techniques of partial correlation analysis [22] and grey relational analysis [23-26] are used to more objectively and quantitatively study the influence of the sidewall and top wall temperatures on the thermal characteristics. In this paper, *Partial Correlation Analysis* was defined as Method 1, and *Grey Relational Analysis* was defined as Method 2. In this article, the *average cooling rate*, *gelatinization layer generation rate at top wall*, and *gelatinization layer generating rate at sidewall* are used to reflect the thermal characteristics during the temperature drop process in the tank. The primary influencing factor was the difference in temperature between top wall and sidewall. There are five simulation cases. Since cooling is a transient thermal process, the quantitative analysis is performed at each moment. In addition, the study results are given as a function of average temperature to make comparisons easier.

– Average cooling rate

Figures 11(a) and 11(b) show the separate effects of sidewall and top wall temperatures on the overall cooling rate of crude. The data in fig. 11(a) were collected based on Method 1, while the data in fig. 11(b) were obtained by Method 2.

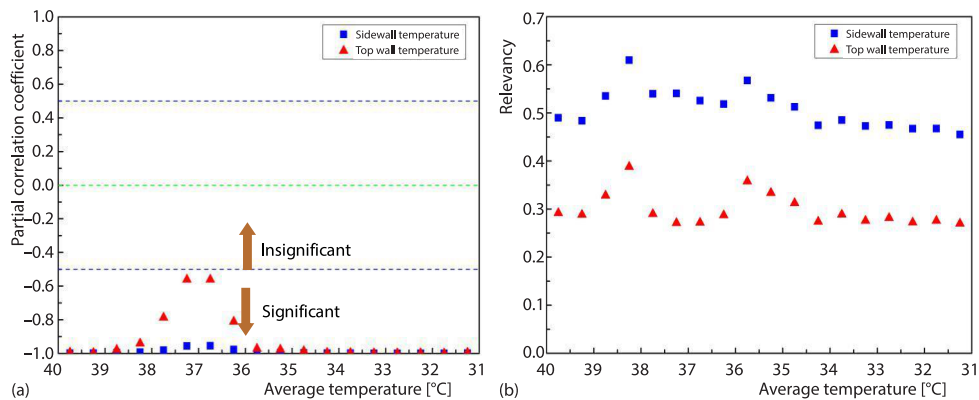


Figure 11. Correlation analysis of the wall temperature and average temperature drop rate; (a) using Method 1 and (b) using Method 2

In Fig. 11(a), using Method 1, the correlation coefficient between sidewall temperature and average temperature drop rate was obtained, and the absolute value was 0.99. Thus, the classification of *strong correlation* can be given. The entire cooling process has a complete *negative correlation* and is very regular, and the wall temperature and average cooling rate are inversely proportional. Similarly, the correlation coefficient between upper wall temperature and average temperature drop rate is 0.92. The *strong correlation* definition is also available. Therefore, the sidewall temperature more greatly affects the average temperature drop rate. The main difference occurs in the temperature range of 38.5-36 °C. Figure 11(b) can be obtained using Method 2, and the same conclusion is also attained. The average relevancy of the sidewall temperature is 0.51, while the average relevancy of the top wall temperature is 0.30.

– Generating rate of the gelatinization layer at the sidewall

Figure 12 shows that the upper boundary temperature and left boundary temperature have independent effects on the formation rate of the sidewall gel layer.

In fig. 12(a), using Method 1, the correlation coefficient between sidewall temperature and generating rate of the gelatinization layer was obtained, and the absolute value was 0.92. The *strong correlation* classification can be defined. The entire cooling process has a complete *negative association*, which is very regular. *Negative correlation* implies that the temperature increase of the sidewall is inversely proportional to the formation rate. The degree of correlation from the top wall temperature to the generation rate is substantially smaller than that from the sidewall to the generation rate. The average partial correlation coefficient in the entire cooling process was calculated, and the absolute value was 0.58. Figure 12(a) shows that there are a *negative correlation* and a *positive correlation* in the cooling process. This result indicates that the upper boundary temperature is independent of the formation rate of the left boundary gel layer, which can be ignored. This hypothesis can be confirmed by the previous discussion.

Figure 12(b) shows that the conclusion obtained by Method 2 is identical to that in fig. 12(a). The left boundary temperature has a greater effect on the gel layer. In addition, the average sidewall temperature relevance is 0.53, while the average top wall temperature is 0.28.

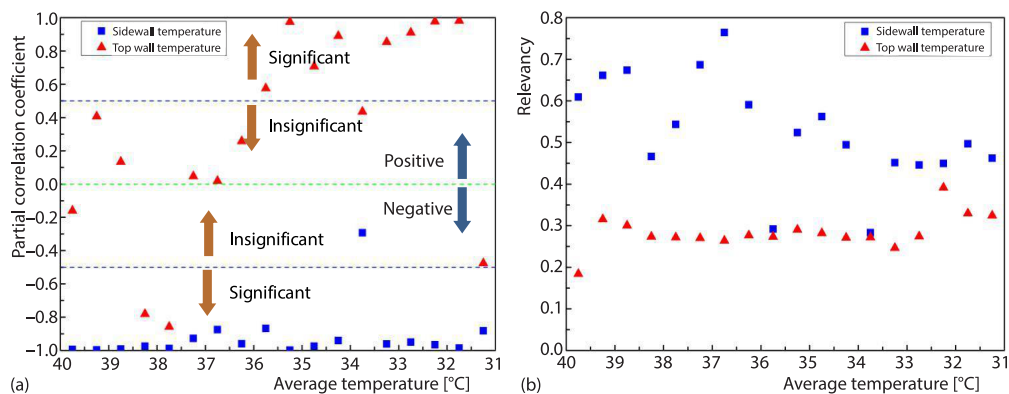


Figure 12. Correlation analysis of the wall temperature and generation rate of the sidewall gelatinized layer; (a) using Method 1 and (b) using Method 2

– Generating rate of the gelatinization layer at the top wall

Figure 13 shows that the upper boundary temperature and left boundary temperature have independent effects on the formation rate of the top wall gel layer.

In fig. 13(a), using Method 1, the correlation coefficient between top wall temperature and generating rate of the gelatinization layer was obtained, and the absolute value was 0.73. Among them, the influence of the top wall temperature is greater and has a certain negative correlation. The mean absolute value of the part-coefficient of correlation between sidewall temperature and top wall gelling layer forming is 0.63. The average temperature change and degree of correlation difference are obvious. Thus, the effect of the sidewall temperature on the generating rate is uncertain and insignificant. The consequence of Method 2 is shown in fig. 13(b). Its overall performance is comparable to that in fig. 13(a). The sidewall temperature has an average relevance of 0.38, while the top wall temperature has an average relevance of 0.42. The effect of the top wall temperature is more significant.

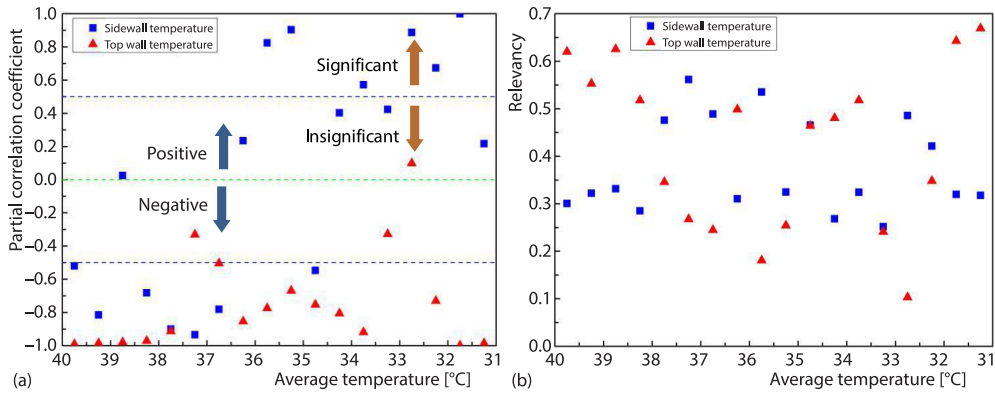


Figure 13. Correlation analysis of the wall temperature and generation rate of the top wall gelatinized layer; (a) using Method 1 and (b) using Method 2

– Data summarization

The relevant data of quantitative analysis are summarized in tab. 1.

Table 1. Data summarization

Concerned physical quantity	Partial correlation coefficient		Average relevancy (Grey relational analysis)	
	Sidewall temperature	Top wall temperature	Sidewall temperature	Top wall temperature
Average cooling rate	0.99	0.92	0.51	0.30
Generating rate of gelatinization layer at sidewall	0.92	0.58	0.53	0.28
Generating rate of gelatinization layer at top wall	0.63	0.73	0.38	0.42

As seen in tab. 1, since the basic theory of two analytical methods is different, the calculated values cannot be directly compared. However, the relative relation is in good agreement. Based on those data, it can be concluded that: during the cooling, the effect of sidewall temperature on the thermal and the derived gelatinization behavior is more significant than that of top wall temperature. They both have the significant influence on the average cooling rate. The largest difference happens when correlating with the generating rate of gelatinization layer at sidewall. The rank of the correlation degree for sidewall temperature is: average cooling rate > generating rate of gelatinization layer at sidewall > generating rate of gelatinization layer at top wall. The rank of the correlation degree for top wall temperature is: average cooling rate > generating rate of gelatinization layer at top wall > generating rate gelatinization layer at sidewall.

Conclusions

- Physical and mathematical models with numerical approaches for the thermal process that represents the static cooling of waxy crude oil were established. Based on the numerical simulation method, the effects of the top wall and sidewall temperatures on the thermal characteristics of waxy crude oil during static cooling were investigated.

- The upper boundary temperature has a major effect on the convective heat transfer and gel layer production rate at the upper wall. Furthermore, the temperature of the oil and temperature differential between crude oil and = upper wall have the opposite effect, and the variation law of the convective heat coefficient and thickness of the gel layer near the upper wall is more complex. In contrast, the upper boundary temperature has no effect on the heat flow characteristics of the temperature drop process and formation rate of the gel layer at the left boundary, and its regularity is obvious. The effect of the sidewall temperature on the convection heat transfer coefficient and gelatinization layer generation rate near the top wall and sidewalls follows the same law.
- In the process of temperature drop, the sidewall temperature has more influence on the heat transfer properties and gel properties. They both significantly affect the average cooling rate. The largest difference occurs when correlating with the generating rate of the gelatinization layer at the sidewall. The association degree for sidewall temperature is ranked the average cooling rate has the highest correlation level, followed by the formation rate of the sidewall cementitious layer, and the smallest is the formation rate of the top wall cementitious layer. The association degree for top wall temperature is ranked the average cooling rate has the largest correlation degree, followed by the generation rate of the top wall gelling layer, and the sidewall rate gelatinization layer has the least degree of correlation.

Nomenclature

C	– constant representing the gelatinous structure	T_{basewall}	– temperature of the basewall, [°C]
C_p	– specific heat of crude oil, [Jkg ⁻¹ C ⁻¹]	T_{roof}	– temperature of the top wall, [°C]
g	– gravitational acceleration, [ms ⁻²]	T_{sidewall}	– temperature of the sidewall, [°C]
H_{tank}	– total height of the computational domain, [m]	T_s	– losing flow temperature of crude-oil, [°C]
h	– convective heat transfer coefficient, [Wm ⁻² C ⁻¹]	T_z	– gelling temperature of crude-oil, [°C]
p	– pressure, [Pa]	t	– cooling time, [second]
p_0	– constant pressure, [Pa]	u	– axial velocity, [ms ⁻¹]
R_{tank}	– diameter of the computational domain, [m]	v	– radial velocity, [ms ⁻¹]
r	– radial co-ordinate, [m]	x	– axial co-ordinate, [m]
S_u	– sink term in the momentum equation	<i>Greek symbols</i>	
S_v	– sink term in the momentum equation	β	– liquid oil percentage, [%]
T	– oil temperature, [°C]	λ	– thermal conductivity of crude-oil, [Wm ⁻¹ C ⁻¹]
		μ	– kinetic viscosity of crude-oil, [Pa·s]
		ρ	– density of crude-oil, [kgm ⁻³]

Acknowledgment

This work is supported by University Nursing Program for Young Scholars with Creative Talents in Heilongjiang Province (UNPYSCT-2018039)

References

- [1] Busson, C., Miniscloux, C., Modele technoeconomique de calorifugeage des reservoirs de fuel lourd (in French), *Rev. Gen. Therm.*, 226 (1980), pp. 785-797.
- [2] Cotter, M. A., Charles, M., Transient Cooling of Petroleum by Natural Convection in Cylindrical Storage Tanks: A Simplified Heat Loss Model, *The Canadian Journal of Chemical Engineering*, 70 (1992), 6, pp. 1090-1093
- [3] Cotter, M. A., Transient Natural Convection in Petroleum Storage Tanks, Ph. D. thesis, University of Toronto, Toronto, Canada, 1991
- [4] Cotter, M. A., Charles, M., Transient Cooling of Petroleum by Natural Convection in Cylindrical Storage Tanks – II, Effect of Heat Transfer Coefficient, Aspect Ratio and Temperature-Dependent Viscosity, *International Journal of Heat and Mass Transfer*, 36 (1993), 8, pp. 2175-2182

- [5] Zhao, B., The Cooling Rule of the Crude Oil in a Storage Tank Based on a New Finite Element Method, *Liquid Fuels Technology*, 31 (2013), 20, pp. 2141-2148
- [6] Zhao B, et al., Application of Gabor Finite Element Method for Oil Tank Stratification in Solar Energy System, *Applied Thermal Engineering*, 107 (2016), Aug., pp. 1130-1137
- [7] Zhao, B., Numerical Simulation for the Temperature Changing Rule of the Crude Oil in a Storage Tank Based on the Wavelet Finite Element Method, *Journal Therm. Anal. Calorim.*, 107 (2012), Mar., pp. 387-393
- [8] Li, W., et al., Numerical Study on Temperature Field of a Large Floating Roof Oil Tank, *CIESC Journal*, 62 (2011), S1, pp. 108-112
- [9] Li, W., Study on Numerical Simulation Methods and Regularities for Temperature Field of Large Floating Roof Oil Tank, Ph. D. thesis, China University of Petroleum, Beijing, China, 2013
- [10] Vardar, N., Numerical Analysis of the Transient Turbulent Flow in a Fuel Oil Storage Tank, *International Journal of Heat and Mass Transfer*, 46 (2003), 18, pp. 3429-3440
- [11] Mawire, A., Experimental and Simulated Thermal Stratification Evaluation of an Oil Storage Tank Subjected to Heat Losses during Charging, *Applied Energy*, 108 (2013), 11, pp. 459-465
- [12] Mawire, A., et al., Experimental Investigation on Simultaneous Charging and Discharging of an Oil Storage Tank, *Energy Conversion and Management*, 65 (2013), 6, pp. 245-254
- [13] Mawire, A., Experimental de-Stratification and Heat Loss in a Storage Tank Containing Different Thermal Oils, *Journal of the Brazilian Society of Mechanical Sciences and Engineering*, 39 (2017), 6, pp. 2279-2288
- [14] Liu, J., et al., Numerical Simulation of Crude Oil Temperature Distribution Near the Tank Wall of 10×10^4 m³ Boating-Roof Tank, *Oil and Gas Storage and Transportation*, 3 (2015), pp. 248-253
- [15] Wang, M., et al., Numerical Study on the Temperature Drop Characteristics of Waxy Crude Oil in a Double-Plate Floating Roof Oil Tank, *Applied Thermal Engineering*, 124 (2017), Sept., pp. 560-570
- [16] Wang, M., et al., Numerical Study on the Temperature Drop Characteristics of Waxy Crude Oil in a Single-Plate Floating Roof Oil Tank, *Petroleum Science Bulletin*, 02 (2017), 2, pp. 267-278
- [17] Wang, M., et al., Experimental and Numerical Study on the Heat Transfer Characteristics of Waxy Crude Oil in a 100000 m³ Double-Plate Floating Roof Oil Tank, *Applied Thermal Engineering*, 136 (2018), May, pp. 335-348
- [18] Zhao, J., et al., Research on Heat Transfer Characteristic of Waxy Crude Oil during the Gelatinization Process in the Floating Roof Tank, *International Journal of Thermal Sciences*, 115 (2017), C, pp. 139-159
- [19] Zhao, J., et al., Numerical Investigation on the Flow and Heat Transfer Characteristics of Waxy Crude Oil during the Tubular Heating, *International Journal of Heat and Mass Transfer*, 161 (2020), 120239
- [20] Zhao, J., et al., Effect of Physical Properties on the Heat Transfer Characteristics of Waxy Crude Oil during Its Static Cooling Process, *International Journal of Heat and Mass Transfer*, 17 (2019), July, pp. 242-262
- [21] Zhao, J., et al., Effect of Geometry of Tank on the Thermal Characteristics of Waxy Crude Oil during Its Static Cooling, *Case Studies in Thermal Engineering*, 1 (2020), 100737
- [22] Shan, Z., Central Limit Theorem of Sample Partial Coefficient, Ph. D. thesis, Northeast Normal University, Changchun, China, 2011
- [23] Celik, N., et al., Application of Taguchi Method and Grey Relational Analysis on a Turbulated Heat Exchanger, *International Journal of Thermal Sciences*, 124 (2018), Feb., pp. 85-97
- [24] Baruah, A., et al., Optimization of AA5052 in Incremental Sheet Forming using Grey Relational Analysis, *Measurement*, 106 (2017), Aug., pp. 106:95-100
- [25] Sun, G., et al., Grey Relational Analysis between Hesitant Fuzzy Sets with Applications to Pattern Recognition, *Expert Systems with Applications*, 92 (2017), Feb., pp. 521-532
- [26] Deng, J. L., Theory and Method of Social and Economic Grey Correlation, *Chinese Social Sciences*, 06 (1984), pp. 47-60